

Calculation of the One-Loop Massive Quark Beam Function in SCET

Report on a Project of the
DESY Summer Student Programme 2015



Anne Spiering, Humboldt-Universität zu Berlin, Germany
supervised by Dr. Piotr Pietrulewicz and Dr. Frank Tackmann

Contents

1	Introduction	1
2	Theoretical Foundations	2
2.1	Factorization of Cross-Sections	2
2.2	Scales and Effective Operators for Initial State Radiation with Massive Quarks	3
2.2.1	$m_b^2 \ll t$	4
2.2.2	$m_b^2 \sim t$	5
2.3	SCET	5
3	Quark PDFs	7
3.1	PDFs in SCET	7
3.2	Tree-Level and 1-Loop Calculation	7
3.3	Matching 5FS onto 4FS	8
4	Quark Beam Functions	9
4.1	Beam Functions in SCET	9
4.2	Tree-Level Calculation	9
4.3	1-Loop Level Calculation	10
5	Matching Beam Functions on PDFs	12
5.1	Tree-Level Matching	12
5.2	One-Loop Matching	13
5.2.1	$\sqrt{t} \gg m_b$	13
5.2.2	$t \sim m_b^2$	14
5.3	Beam Function for Arbitrary Hierarchies between m_b and \sqrt{t}	15
5.4	Main Results of this Report	16

Chapter 1

Introduction

One approach in the search for new physics is to probe the Standard Model (SM) of elementary particle physics in high-energy experiments like hadron colliders. There, new physics is expected to show up at very short distances, i.e. high energies. In order to judge whether experimental data point towards physics beyond the SM, one has to provide precise theoretical predictions for these experiments within the framework of the SM. Due to the hadronic initial states, experimental cuts etc. these processes are multi-scale processes which require to describe them within factorization framework. Restricting the initial state contribution e.g. by a jet veto implies that the whole initial state is not merely described by parton distribution functions (PDFs) of the colliding hadrons but rather by the so called beam functions characterizing the initial state jets. This report shall discuss the question of how to incorporate massive quark effects in these objects theoretically.

First of all we will give a short review on some of the theoretical background in chapter 2. Afterwards we define operators describing the initial state radiation at the jet veto scale and calculate gluon matrix elements of the partonic PDF and the partonic beam function operator. We conclude this report with the result for matching corrections between these effective operators in chapter 5.

Chapter 2

Theoretical Foundations

This chapter shall give a small glimpse at some of the theory behind the calculation of initial states in hadron-hadron collisions. The first section summarizes how to disentangle the contributions of the initial state from the rest of the physics in the cross section. This part is mainly based on [1]. Then we will discuss the steps in a calculation of a beam function starting from the PDF of a proton exploiting the physics behind the initial state at different energy scales (mainly based on [2] and [3]). Eventually there will be a short review on soft-collinear effective theory (SCET) on the basis of [4] and [5].

2.1 Factorization of Cross-Sections

The goal of all theoretical calculations in physics is to obtain physical quantities that can be checked experimentally in order to verify or falsify the underlying theory. Within the context of collider experiments this quantity is the cross section σ of a specific process given as a function of leptonic or hadronic observables. Because of the presence of multiple scales in these experiments it is often useful to disentangle the corresponding physics in its calculation, such as the universal nonperturbative physics at low energies and the process dependent perturbative physics at higher energies. This concept is called *factorization* and will be explained in the following.

The standard factorization theorem for a fully inclusive collision of two hadrons is

$$d\sigma = f \otimes f \otimes H_{incl} \quad (2.1)$$

where f denotes the PDF which gives the probability of finding a specific parton with specific momentum fraction inside each of the colliding hadrons and H_{incl} is the perturbatively calculable partonic cross-section of the considered hard interaction. Thus, the calculation of the cross section reduces to a calculation of the initial-state PDFs f and H_{incl} incorporating all contributions of the hard scattering process.

This factorization theorem is probably the easiest but is only suitable for experimental setups where one has no restriction on the final state or any hard physics. In contrast to this, final states of most experiments are restricted by constraints and cuts on certain kinematic variables due to the apparatus, statistics and to identify decay chains with certain properties of the final state, e.g. specific numbers of hard jets, leptons and photons or energy limits. In order to set up theoretical predictions for these experimental observables ("fiducial cross-sections") one has to apply suitable factorization theorems.

Introducing a jet veto, e.g. by restricting the invariant mass $p^2 = -t$ of the beams to be $t \ll Q^2$, where Q is the momentum transfer during the hard interaction, leads to a sensitivity on collinear scales at $\sim \sqrt{t}$ and soft scales at $\sim \frac{t}{Q}$ and a factorization theorem in the form of

$$d\sigma = H \cdot \left(\prod_i J_i \cdot B \cdot B \right) \otimes S \left[1 + \mathcal{O} \left(\frac{t}{Q^2} \right) \right] \quad \text{with } B = \mathcal{I} \otimes f \left[1 + \mathcal{O} \left(\frac{\Lambda_{QCD}^2}{t} \right) \right] \quad (2.2)$$

which can be derived using SCET discussed in chapter 2.3. It is a convolution of different functions:

- f is the PDF of each colliding proton associated to a low hadronic scale $\mu_\Lambda \sim \Lambda_{QCD}$
- \mathcal{I} takes into account the initial-state radiation of the partons prior to the hard collision at the veto scale $\mu_B \sim \sqrt{t}$
- H is the perturbative function describing the hard interaction of the scattering event at $\mu_H \sim Q$
- J_i describes the different final-state jets at $\mu_J \sim m_J$ with m_J as invariant mass of the jets
- S includes the impact of wide-angle soft gluons radiated from the energetic strongly interacting particles at $\mu_S \sim \frac{t}{Q}$.

Thus the initial-state is not only described by the probability density f of extracting a specific parton but also by the initial radiation which changes the virtuality t of the parton and is incorporated in the function \mathcal{I} . Thus the initial-state proton is replaced by a jet of partons not constrained to remain inside the proton anymore. Both components together are described by the beam function $B = \mathcal{I} \otimes f$.

A hierarchy of these scales results in large logarithms of the ratios of the scales in perturbation theory which have to be resummed to obtain precise predictions for the cross section.

2.2 Scales and Effective Operators for Initial State Radiation with Massive Quarks

After having separated different physical contributions to the cross section in a collider experiment we will now concentrate on the initial state of the collision process described by the beam function and investigate how factorization works out for these contributions when massive quarks are present. This discussion is relevant e.g. in deep inelastic scattering and can be extended for hadron-hadron collisions such as in the $b\bar{b}H$ -process (see [3]).

For the calculation of the beam function at the scale $\mu_B \sim \sqrt{t}$ one has to consider all the physics of the lower scales beginning with the nonperturbative PDFs and match between different effective field operators describing the physics in intermediate regimes with new scales such as the mass of the heavy b -quark $\mu_m \sim m_b$ and at $\mu_B \sim \sqrt{t}$. A hierarchy between these scales again introduces large logarithms of their ratios in the perturbative results leading to a slow convergence of the fixed-order perturbative series. A resummation of these logarithms can be achieved using evolution equations discussed in the following.

During the discussion of the computation of beam functions we will differentiate the following two cases:

1. $m_b^2 \ll t$: $\mu_\Lambda \ll \mu_m \ll \mu_B$
2. $m_b^2 \sim t$: $\mu_\Lambda \ll \mu_m \sim \mu_B$.

Thus we will always assume $m_b \gg \Lambda_{QCD}$ because otherwise we cannot describe the b -quark perturbatively.

2.2.1 $m_b^2 \ll t$

Let us first discuss the case where there is more hierarchal structure. At a low energy scale $\mu_\Lambda \gtrsim \Lambda_{QCD}$ which separates nonperturbative and perturbatively calculable physics the initial state physics can be described by the light quarks u, d, s, c and gluons only¹, the heavy quarks b and t are treated as decoupled, i.e. all interactions with momentum transfer $\gtrsim m_b$ are integrated out. The associated PDFs in this so-called 4-flavor-scheme (4FS) effective theory, where the heavy quarks are integrated out and the light quarks are taken to be massless, are denoted by $f_i^{[4]}(\xi, \mu_\Lambda)$ and give the probability of finding one of the light partons i with momentum fraction ξ inside the proton. The dependence on the momentum fraction is non-perturbative because of the large coupling between the partons inside the proton and thus has to be determined using experimental data. The perturbative evolution of the PDFs from μ_Λ to higher scales μ is possible using the renormalization group evolution (RGE) equations for $k = 4$

$$\mu \frac{d}{d\mu} f_i^{[k]}(\xi, \mu) = \int \frac{d\xi'}{\xi'} \gamma_{ij}^{[k]} \left(\frac{\xi}{\xi'}, \mu \right) f_j^{[k]}(\xi', \mu). \quad (2.3)$$

These so-called DGLAP equations include the anomalous dimension $\gamma_{ij}^{[k]}$ given perturbatively by the well-known Altarelli-Parisi splitting functions. They mix the different partons, redistribute their momentum fractions and resum single logarithms of the ratio of μ and μ_Λ if $f_i^{[4]}(\xi, \mu_\Lambda)$ is set as initial condition.

This evolution stops at the scale μ_m where the massive b quark starts to be treated as dynamic flavor and can be pair-produced, so altogether there are 5 active flavors which can strongly interact. In order to pass over from the 4FS to the 5-flavor scheme (5FS) one matches the 5-flavor theory onto the 4-flavor theory by a factorization

$$f_i^{[5]}(m_b, \mu_m) = \mathcal{M}_{ij}(m_b, \mu_m) \otimes f_j^{[4]}(\mu_m) \left[1 + \mathcal{O} \left(\frac{\Lambda_{QCD}^2}{m_b^2} \right) \right] \quad (2.4)$$

with $i \in \{u, d, c, s, b, g\}$ whereas $j \in \{u, d, c, s, g\}$. Thus, all effects of the b -quark will be captured inside the m_b -dependent Wilson (matching) coefficients \mathcal{M}_{ij} . The operator \otimes denotes the convolution

$$(\mathcal{M}_{ij} \otimes f_j^{[4]})(\xi) = \int_\xi^1 \frac{dz}{z} \mathcal{M}_{ij} \left(\frac{\xi}{z} \right) f_j^{[4]}(z) \quad (2.5)$$

¹Depending on the application it is also possible to decouple the c -quark at first, only determine the nonperturbative PDF for the u, d and s quarks and afterwards include the c -quark perturbatively by matching onto a theory with a heavy c -quark.

which mixes the different partons and redistributes their momentum fractions. This matching can be performed perturbatively until the desired number of orders is achieved.

The PDFs $f_i^{[5]}(m_b, \xi, \mu_m)$ can be evolved using the standard PDF DGLAP-evolution equations (2.3) for $k = 5$. If $f_i^{[5]}(m_b, \xi, \mu_m)$ are chosen as initial conditions, the evolution will resum single logarithms of $\frac{\mu}{\mu_m}$.

At the scale $\mu_B \sim \sqrt{t}$ this evolution stops since a new physical scale appears: The partons emit collinear (and soft) radiation which pushes the partons off-shell with virtuality t . These contributions with momentum transfer $\gtrsim \sqrt{t}$ were integrated out in the 5FS. The resulting jet-like structure of collinear partons and gluon radiation can be described by beam functions $B_i(t, x, \mu)$ where $i \in \{u, d, c, s, b, g\}$. Again the transition between both effective operators is performed by a matching equation

$$B_i(t, m_b, \mu_B) = \mathcal{I}_{ij}^{[5]}(t, \mu_B) \otimes f_j^{[5]}(m_b, \mu_B) \left[1 + \mathcal{O}\left(\frac{m_b^2}{t}\right) \right] \quad (2.6)$$

with perturbatively calculable Wilson (matching) coefficients \mathcal{I}_{ij} including all effects of the emitted radiation such as the change of the momentum fraction from ξ to x and of the identity due to pair-production or gluon emission. The expansion in $\frac{m_b^2}{t}$ implies that the LO term of $\mathcal{I}_{ij} \forall i, j$ will be independent of m_b .

The evolution of the beam function is governed by the RGE

$$\mu \frac{d}{d\mu} B_i(t, x, \mu) = \int dt' \gamma_B^i(t - t', \mu) B_i(t', x, \mu) \quad (2.7)$$

with anomalous dimensions γ_B^i . This evolution does not mix the different parton species and leaves the momentum fraction x unchanged. Furthermore it resums Sudakov double logarithms of the ratio $\frac{\mu}{\sqrt{t}}$ giving collinear singularities for $t \rightarrow 0$.

This evolution can be performed until it reaches the hard scale μ_H associated with the momentum transfer Q during the hard interaction. Since we set $\mu_H \ll m_t$ with the top mass m_t , the t -quarks are still decoupled.

2.2.2 $m_b^2 \sim t$

In contrast to this, there is only one matching step needed in the second case. Because of the coincidence of the scales μ_m and μ_B one can directly match the beam function B_i at $\mu_B \sim m_b \sim \sqrt{t}$ onto the 4FS PDFs $f_i^{[4]}$ evolved to this scale:

$$B_i(t, m_b, \mu_B) = \mathcal{I}_{ij}^{[4]}(t, m_b, \mu_B) \otimes f_j^{[4]}(\mu_B) \left[1 + \mathcal{O}\left(\frac{\Lambda_{QCD}^2}{t^2}\right) \right] \quad (2.8)$$

where $j \in \{u, d, s, c, g\}$ whereas $i \in \{u, d, s, c, b, g\}$. Thus all fluctuations in the order of m_b and t are integrated out in a single matching step.

2.3 SCET

Before proceeding with an explicit calculation of beam functions let us discuss an effective field theory of QCD called SCET which enables us to focus only on the relevant degrees of freedom in this problem. Since we discuss processes including collinear incoming partons emitting collinear and soft radiation this framework is

particularly suitable because it integrates out all higher invariant mass contributions and resums large logarithms resulting from the IR behavior related to soft and collinear momenta. Furthermore, SCET gives well-defined gauge-independent definitions of the PDF and beam function in terms of operator matrix elements of the relevant fields.

In the discussed interaction process the direction of the collinear parton interacting strongly is of great importance and working in coordinates adjusted to this direction can help us reveal hierarchies in the momenta. Hence we introduce light-like vectors n^μ and \bar{n}^μ defined as

$$n^\mu = (1, 0, 0, 1) \quad \bar{n}^\mu = (1, 0, 0, -1) \quad n^2 = \bar{n}^2 = 0 \quad n \cdot \bar{n} = 2 \quad (2.9)$$

and align the collinear partons and radiation in the initial state jet with the $\vec{z} = \vec{n} = (0, 0, 1)$ beam direction. Then each momentum can be decomposed as

$$p^\mu = \bar{n} \cdot p \frac{n^\mu}{2} + n \cdot p \frac{\bar{n}^\mu}{2} + p_\perp^\mu \equiv (p^+, p^-, \vec{p}_\perp) \quad (2.10)$$

where $p_\perp^\mu = (0, p^1, p^2, 0)$ describes all the momentum components orthogonal to n^μ and \bar{n}^μ and \vec{p}_\perp is the two-dimensional euclidean of p_\perp^μ with $\vec{p}_\perp^2 = -p_\perp^2$ using the mostly minus Minkowski metric. Additionally it is $p^+ \equiv n \cdot p$ and $p^- \equiv \bar{n} \cdot p$. In these coordinates the invariant mass can be written as

$$p^2 = p^+ p^- - \vec{p}_\perp^2. \quad (2.11)$$

In order to describe soft and collinear modes and their hierarchy in momentum components we furthermore need a high and low scale. All momenta with invariant mass of the order of the hard scale are integrated out whereas the momenta with invariant mass close to the low scale are described within SCET as soft or collinear momenta. For the calculation of the beam function we will use SCET in the limit $t \ll Q^2$ and thus we can define a power counting parameter $\lambda \sim \frac{\sqrt{t}}{Q}$. Then collinear momenta in the n - and \bar{n} -direction scale as

$$p_n^\mu \sim Q_h(1, \lambda^2, \lambda) \quad p_{\bar{n}}^\mu \sim Q_h(\lambda^2, 1, \lambda). \quad (2.12)$$

In this report we will investigate soft modes scaling as

$$p_{us}^\mu \sim Q_h(\lambda^2, \lambda^2, \lambda^2) \quad (2.13)$$

often denoted as ultrasoft in order to differentiate between the here used SCET-I and SCET-II with a different scaling for soft modes.

In the following we will deal with collinear quarks and gluons in the initial state jet. Using the framework of SCET-I one can decompose the Lagrangian of QCD in collinear and soft contributions and obtain the following Feynman rules

- collinear quark propagator with momentum p , mass m and large p^- component

$$i \not{n} \frac{\bar{n} \cdot p}{2 (n \cdot p)(\bar{n} \cdot p) + p_\perp^2 - m^2 + i0} = i \not{n} \frac{\bar{n} \cdot p}{2 p^2 - m^2 + i0} \quad (2.14)$$

- vertex of a collinear gluon with momentum k and a collinear quark with mass m , incoming momentum $p + k$ and outgoing p

$$igt^a V_n^\mu(p, p+k, m) = igt^a \left[n^\mu + \gamma_\perp^\mu \frac{(\not{p} + \not{k})_\perp + m}{\bar{n} \cdot (p+k)} + \frac{\not{p}_\perp - m}{\bar{n} \cdot p} \gamma_\perp^\mu - \frac{(\not{p}_\perp - m)((\not{p} + \not{k})_\perp + m)}{(\bar{n} \cdot k)(\bar{n} \cdot (p+k))} \bar{n}^\mu \right]. \quad (2.15)$$

Chapter 3

Quark PDFs

3.1 PDFs in SCET

Since beam functions contain PDF-effects we first discuss the calculation of some PDFs which is based on techniques used in [2] and [3]. In SCET they are defined as the nonperturbative proton matrix elements

$$f_i(\mu) = \langle p | \mathcal{Q}_i(\mu) | p \rangle \quad (3.1)$$

of the PDF operator \mathcal{Q}_i where i denotes the parton initiating the hard interaction and $|p\rangle$ the external proton state.

In this report we will only consider diagrams with gluons in the external state and restrict ourselves to quark-initiated contributions at 1-loop level. The corresponding partonic PDF is

$$f_{q/g}(\xi, \mu) = \langle g(p^-) | \mathcal{Q}_q(\omega, \mu) | g(p^-) \rangle. \quad (3.2)$$

Here $p^- = \bar{n} \cdot p$ is the collinear momentum of the incoming gluon which shall have no perpendicular momentum \vec{p}_\perp . ω is the minus-component of the momentum flowing into the initial state jet initiating interaction (called hard in the following because these interactions have a momentum transfer which is integrated out) and ξ is the ratio $\xi = \frac{\omega}{p^-}$. The bare quark operator is

$$\mathcal{Q}_q^{bare}(\omega) = \theta(\omega) \bar{\chi}_n(0) \frac{\not{n}}{2} [\delta(\omega - \bar{n} \cdot \mathcal{P}_n) \chi_n(0)] \quad (3.3)$$

where χ_n is the SCET field of n collinear quarks depending on the position in space y^μ and $\bar{\chi}_n$ is the corresponding collinear antiquark field. \mathcal{P}_n is the momentum operator and the square-bracket denotes that $\delta(\omega - \bar{n} \cdot \mathcal{P}_n)$ only acts inside it.

3.2 Tree-Level and 1-Loop Calculation

At leading order, the collinear parton i with momentum fraction ξ in the initial state simply does the hard interaction itself. For an incoming collinear quark such a contribution to the hard interaction process is illustrated in Figure 3.1 and for a collinear gluon in Figure 3.2. Dashed lines represent collinear quarks, springs with lines denote collinear gluons and the crossed vertex is the hard interaction vertex.

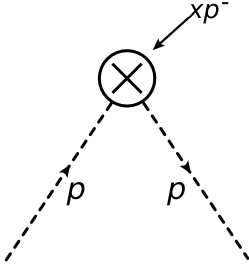


Figure 3.1: LO diagram for a quark-initiated hard interaction

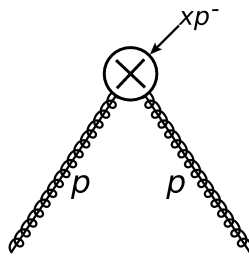


Figure 3.2: LO diagram for a gluon-initiated hard interaction

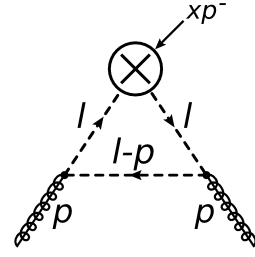


Figure 3.3: NLO diagram for a quark-initiated hard interaction with gluons in the external state

The partonic PDF for this process using (3.3) is simply given by

$$f_{i/j}^{(0)}(\xi, \mu) = \delta_{ij} \theta(\xi) \delta(1 - \xi). \quad (3.4)$$

The first factor denotes that there is only a non-vanishing tree-level term for $i = j$, i.e. incoming and strongly interacting parton are the same. The second term trivially implies that the momentum fraction of the scattered parton has to be positive and the last factor emphasizes that the strongly-interacting parton carries all the momentum of the incoming parton at tree-level.

At NLO we only consider contributions of quark-initiated strong interactions with gluons in the external state. The corresponding diagram is shown in Figure 3.3. Applying the definition (3.3) and SCET Feynman rules (2.14) and (2.15), using dimensional regularization and contour integration we obtain for a massless fermion loop the well-known result

$$f_{q/g}^{(1)bare}(\xi, \mu) = \frac{\alpha_s(\mu) T_F}{2\pi} \theta(\xi) \left\{ \left[\frac{1}{\epsilon} - \log \frac{t'(1-\xi)}{\mu^2} \right] P_{gq}(\xi) - \theta(1-\xi) \right\} \quad (3.5)$$

with the splitting function

$$P_{gq}(\xi) = \theta(1-\xi)(1-2\xi+2\xi^2). \quad (3.6)$$

This expression is UV-divergent which is encoded in the $\frac{1}{\epsilon}$ -term and IR-divergent for $t' = -\omega p^+ \rightarrow 0$ with small $p^+ < 0$.

The diagram with massive fermion loop yields

$$f_{b/g}^{(1)bare}(\xi, \mu) = \frac{\alpha_s(\mu) T_F}{2\pi} \theta(\xi) \left\{ \left[\frac{1}{\epsilon} - \log \frac{m_b^2}{\mu^2} \right] P_{gq}(\xi) \right\}. \quad (3.7)$$

3.3 Matching 5FS onto 4FS

Matching the renormalized 5FS partonic PDFs onto the 4FS partonic PDFs using equation (2.4) yields the following well-known matching coefficients at LO

$$\mathcal{M}_{gg}^{(0)}(\xi) = \mathcal{M}_{qq}^{(0)}(\xi) = \delta(1-\xi) \quad \mathcal{M}_{gq}^{(0)}(\xi) = \mathcal{M}_{qg}^{(0)}(\xi) = \mathcal{M}_{bq}^{(0)}(\xi) = \mathcal{M}_{bg}^{(0)}(\xi) = 0 \quad (3.8)$$

and at NLO

$$\mathcal{M}_{gg}^{(1)}(\xi, m_b, \mu_m) = f_{g/g}^{[5](1)} - f_{g/g}^{[4](1)} = -\frac{\alpha_s}{\pi} \frac{4T_F}{3} \log \frac{\mu_m^2}{m_b^2} \delta(1-\xi) \quad (3.9)$$

$$\mathcal{M}_{bg}^{(1)}(\xi, m_b, \mu_m) = f_{b/g}^{[5](1)} = \frac{\alpha_s}{2\pi} T_F \theta(\xi) P_{gq}(\xi) \log \frac{\mu_m^2}{m_b^2}. \quad (3.10)$$

Chapter 4

Quark Beam Functions

4.1 Beam Functions in SCET

Analogously to PDFs, SCET beam functions are defined as proton matrix elements of the beam function operator \mathcal{O}_i :

$$B_i(t, x, \mu) = \langle p | \theta(\omega) \mathcal{O}_i(t, \omega, \mu) | p \rangle. \quad (4.1)$$

Similar to the last chapter we will only consider diagrams with gluons in the external states and restrict ourselves to quark-initiated contributions at NLO. The corresponding beam function reads

$$B_{q/g}(t, x, \mu) = \langle g(p^-) | \theta(\omega) \mathcal{O}_q(t, \omega, \mu) | g(p^-) \rangle \quad (4.2)$$

with incoming large gluon momentum p^- . Here $t = \omega b^+$ is the virtuality of the strongly-interacting parton with minus momentum $x p^- = \omega$ and plus momentum $-b^+$.

In SCET this quark beam function operator is given by the Fourier transform of

$$\tilde{\mathcal{O}}_q^{bare}(y^-, \omega) = e^{-\frac{i}{2} \hat{p}^+ y^-} \bar{\chi}_n \left(y^- \frac{n}{2} \right) \frac{\overrightarrow{\not{n}}}{2} \left[\delta(\omega - \bar{\mathcal{P}}_n) \chi_n(0) \right] \quad (4.3)$$

which includes the plus momentum operator \hat{p}^+ and (anti-)quark fields at positions $y^\mu = y^- \frac{n^\mu}{2}$ and 0. This separation in the y^- component makes the operator non-local. Fourier transformation yields

$$\mathcal{O}_q^{bare}(|\omega| b^+, \omega) = \bar{\chi}_n(0) \delta(\omega b^+ - \omega \hat{p}^+) \frac{\overrightarrow{\not{n}}}{2} \left[\delta(\omega - \bar{\mathcal{P}}_n) \chi_n(0) \right]. \quad (4.4)$$

4.2 Tree-Level Calculation

The beam function tree-level diagrams are shown in Figure 4.1 and 4.2. The incoming quark or gluon simply proceeds to the hard interaction with momentum transfer Q whose vertex is two-parted due to the nonlocality of the beam function operator and afterwards the quark or gluon directly continues to the final state.

Using the definition of the beam function in (4.2) and (4.4) one obtains the tree-level result

$$B_{i/j}^{(0)}(t, x, \mu) = \delta_{ij} \theta(x) \delta(1-x) \delta(t) \quad (4.5)$$

similar to the partonic PDF result. The δ -function in t indicates that this process takes place without any initial-state radiation and thus, the partons have no virtuality at tree level.

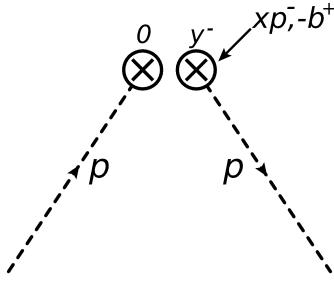


Figure 4.1: Tree-level diagram for a quark-initiated hard interaction

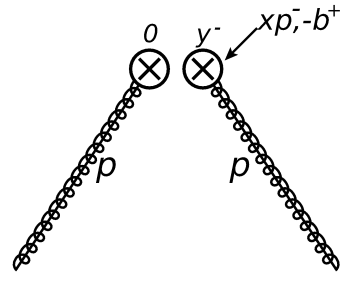


Figure 4.2: Tree-level diagram for a gluon-initiated hard interaction

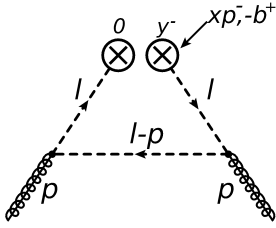


Figure 4.3: 1-Loop diagram for a quark-initiated hard interaction with gluon external state

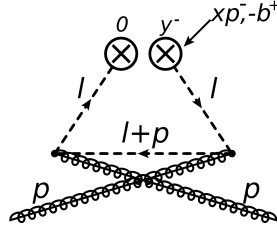


Figure 4.4: 1-Loop diagram for a quark-initiated hard interaction with gluon external state

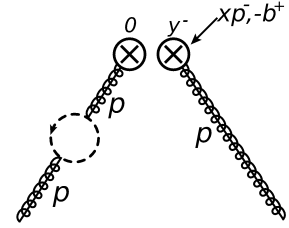


Figure 4.5: 1-Loop diagram for a gluon-initiated hard interaction with gluon external state

4.3 1-Loop Level Calculation

In general there are two different kinds of beam function diagrams. On the one hand one has disconnected diagrams, i.e. the two external states are not connected by propagators and vertices (e.g. tree-level diagrams) and on the other hand there are connected diagrams (e.g. NLO-diagrams with gluons as external states). The latter can be calculated using

$$\langle g | \theta(\omega) \mathcal{O}_q(t, \omega) | g \rangle_{connected} = \text{Disc}_{t>0} \langle g | T_q(t, \omega) | g \rangle \quad (4.6)$$

where Disc denotes the discontinuity of the inserted function and $\langle g | T_q(t, \omega) | g \rangle$ is the time-ordered gluon matrix-element for this process which can be calculated using the SCET Feynman rules. The discontinuity of real functions is given by

$$\text{Disc } g(x) = 2i \text{Im}(g(x + i0)). \quad (4.7)$$

The NLO-diagrams with gluons in the external states are shown in Figures (4.3) and (4.4). A calculation of the first diagram yields the well-known result

$$B_{q/g}^{(1)}(t, x, \mu) = \frac{\alpha_s(\mu)}{2\pi} T_F \theta(x) P_{qg}(x) \frac{\theta(t)t}{(t + xt')^2}. \quad (4.8)$$

$t' = -\omega p^+$ regulates the IR divergence with small $p^+ < 0$. The diagram has no UV-divergent term which ensures that renormalization does not mix \mathcal{O}_q and \mathcal{O}_g confirming that (2.7) does not mix beam functions associated to different partons.

The second 1-loop diagram can be calculated using the result in (4.8) by replacing $p^\mu \rightarrow -p^\mu$ and therefore $z \rightarrow -z$ and $z < 0$. This is contrary to the factor $\theta(z)$ obtained during the calculation of the discontinuity and thus this beam function diagram vanishes.

We will now calculate the diagram in Figure 4.3 for a massive fermion loop more explicitly. Since we already know that this diagram must be UV finite we calculate it without any UV regulator right from the beginning. Using the SCET Feynman rules gives

$$\begin{aligned}
B_{Q/g}^{(1)}(t, x, \mu) &= \text{Disc}_{t>0} \left[-\bar{\epsilon}_\mu(p) \int \frac{d^4 l}{(2\pi)^4} \text{tr} \left[\left(i g t^a \frac{\not{l}}{2} V_n^\mu(l-p, l, m) \right) \right. \right. \\
&\quad \cdot \left(i \frac{\not{l}}{2} \frac{l^-}{l^2 - m^2 + i0} \right) \cdot \delta(l^- - x p^-) \delta(l^+ + b^+ - p^+) \frac{\not{l}}{2} \cdot \\
&\quad \cdot \left(i \frac{\not{l}}{2} \frac{l^-}{l^2 - m^2 + i0} \right) \cdot \left(i g T^b \frac{\not{l}}{2} V_n^\nu(l, l-p, m) \right) \\
&\quad \cdot \left. \left(i \frac{\not{l}}{2} \frac{l^- - p^-}{(l-p)^2 - m^2 + i0} \right) \frac{\theta(z p^-)}{z p^-} \right] \\
&= i g^2 T_F (-\bar{\epsilon}_\mu \epsilon_\nu) \text{Disc}_{t>0} \left[\int \frac{d^4 l}{(2\pi)^4} \frac{1}{2} \text{tr} [V_n^\mu(l-p, l, m) V_n^\nu(l, l-p, m)] \cdot \right. \\
&\quad \cdot \frac{(l^-)^2 (l^- - p^-)}{(l^2 - m^2 + i0)^2 ((l-p)^2 - m^2 + i0)} \cdot \\
&\quad \cdot \left. \delta(l^- - x p^-) \delta(l^+ + b^+ - p^+) \frac{\theta(z p^-)}{z p^-} \right].
\end{aligned}$$

The l^+ - and l^- -integration is performed using the δ -distributions which yields

$$\begin{aligned}
&= -i \frac{\alpha_s}{2\pi^2} T_F \frac{\theta(x)}{x(1-x)} \text{Disc}_{t>0} \left[\int_0^\infty d|\vec{l}_\perp| \right. \\
&\quad \left. \frac{(1-2x+2x^2)|\vec{l}_\perp|^3 + m^2|\vec{l}_\perp|}{(|\vec{l}_\perp|^2 + t + t' + m^2)^2 (|\vec{l}_\perp|^2 - \frac{1-x}{x}t + m^2)} \right] \\
&= i \frac{\alpha_s}{4\pi^2} T_F \theta(x) \text{Disc}_{t>0} \left[\left((1-2x+2x^2)t + 2m^2x^2 \right) \frac{\log \left(m^2 - \frac{1-x}{x}t \right)}{(t + xt')^2} \right]
\end{aligned}$$

These nontrivial discontinuities can be calculated using

$$\frac{i}{2\pi} \text{Disc} \frac{1}{x} = \delta(x) \quad \text{Disc} \log x = 2\pi i \theta(-x) \quad (4.9)$$

and thus we obtain

$$\begin{aligned}
&= \frac{\alpha_s}{2\pi} T_F \theta(x) \theta(1-x) \left[(1-2x+2x^2)t + 2m^2x^2 \right] \frac{\theta \left(\frac{1-x}{x}t - m^2 \right)}{(t + xt')^2} \\
&= \frac{\alpha_s}{2\pi} T_F \theta(x) \left[P_{gq}(x)t + 2m^2\theta(1-x)x^2 \right] \frac{\theta \left(\frac{1-x}{x}t - m^2 \right)}{t^2}. \quad (4.10)
\end{aligned}$$

where we removed the IR-regulator t' because the result is IR-safe due to the mass m_b (we could have also neglected t' right from the beginning).

Another NLO massive 1-loop diagram is illustrated in 4.5. Its contribution can be directly obtained from (3.9)

$$B_{g/g}^{(1)}(t, m_b, x, \mu) \Big|_{ML} = -\frac{\alpha_s}{\pi} \frac{4T_F}{3} \delta(t) \log \frac{\mu^2}{m_b^2} \delta(1-x) \quad (4.11)$$

where the index ML shall emphasise that this is only the contribution of the massive loop.

Chapter 5

Matching Beam Functions on PDFs

In order to pass from PDFs that describe partons inside hadrons in the initial state to beam functions describing jets of collinear partons and radiated gluons one has to match the associated operators at the scale μ_B . First we will do the tree-level matching and afterwards perform the matching at NLO for the aforementioned cases $\sqrt{t} \sim m_b$ and $\sqrt{t} \gg m_b$. We also discuss how the beam function matching can be written for general hierarchies between m_b and \sqrt{t} by including the nonsingular terms in $\frac{m_b}{\sqrt{t}}$ to the 5-flavor resummation result.

5.1 Tree-Level Matching

The matching equation for beam functions and partonic PDFs at tree-level

$$B_{i/k}^{(0)}(t, x, \mu_B) = \mathcal{I}_{ij}^{(0)}(t, \mu_B) \otimes f_{j/k}^{(0)}(\mu_B) = \mathcal{I}_{ik}^{(0)}(t, x, \mu_B) \quad (5.1)$$

yields

$$\mathcal{I}_{ik}^{(0)}(t, x, \mu_B) = \delta_{ik} \theta(x) \delta(1-x) \delta(t). \quad (5.2)$$

Thus the transition from partonic PDFs to beam functions at tree-level is given by

$$B_{i/k}^{(0)}(t, x, \mu_B) = \delta(t) f_{i/k}^{(0)}(x, \mu_B) \quad (5.3)$$

which is illustrated for a gluon initiated hard interaction in Figure 5.1.

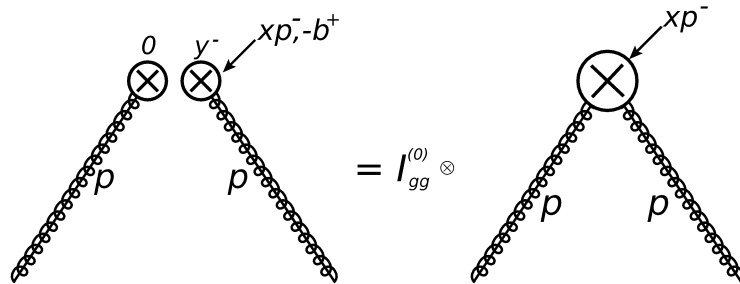


Figure 5.1: Tree-level matching between beam functions and partonic PDFs for gluon initiated hard interactions

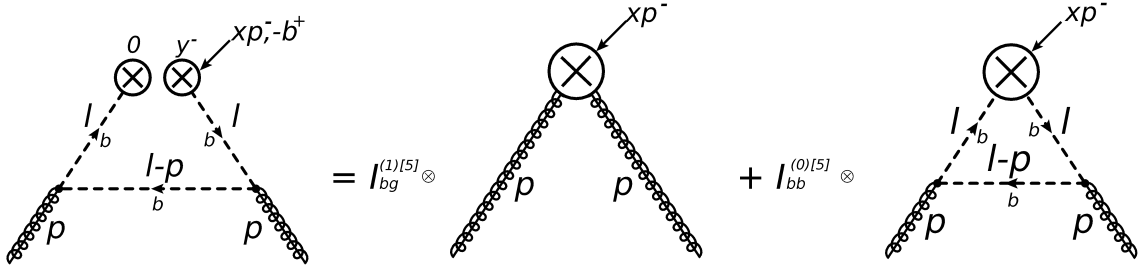


Figure 5.2: NLO matching between beam functions and 5FS partonic PDFs for heavy-quark initiated hard interactions with gluons in the external state

5.2 One-Loop Matching

5.2.1 $\sqrt{t} \gg m_b$

Now we come to the matching at NLO. For $\sqrt{t} \gg m_b$ we match the beam function onto the partonic PDF in the 5FS at $\mu_B \sim \sqrt{t}$. Considering only heavy-quark initiated hard interactions with gluons in the external states yields the NLO matching equation

$$\begin{aligned} B_{b/g}^{[5](1)}(t, m_b, \mu_B) &= \mathcal{I}_{bi}^{(0)[5]}(t, m_b, \mu_B) \otimes f_{i/g}^{(1)[5]}(m_b, \mu_B) + \mathcal{I}_{bi}^{(1)[5]}(t, \mu_B) \otimes f_{i/g}^{(0)[5]}(\mu_B) \\ &= \delta(t) f_{b/g}^{(1)[5]}(m_b, \mu_B) + \mathcal{I}_{bg}^{[5](1)}(t, m_b, \mu_B) \end{aligned}$$

which is illustrated in Figure 5.2 and where the subscript [5] is introduced in order to differentiate between the different results for $\sqrt{t} \gg m_b$ and $\sqrt{t} \sim m_b$. The sum over the index i is over the light quarks, gluons and the b quark. In the first term only $i = b$ contributes whereas the second one is only nonvanishing for $i = g$. Since this equation is only valid up to $\mathcal{O}\left(\frac{m_b^2}{t}\right)$ we expand all terms in ratios of $\frac{m_b^2}{t}$. The partonic PDF $f_{b/g}^{(1)[5]}(x, \mu_B)$ given in (3.7) only contains terms $\mathcal{O}\left((m_b^2 t^{-1})^0\right)$.

In the limit $m_b \rightarrow 0$ distributive structures appear in the beam function $B_{b/g}^{[5](1)}(t, x, \mu_B)$. In order to extract them we need the plus-distribution $\frac{1}{\mu^2} \mathcal{L}_0 \left[\frac{t}{\mu^2} \right] = \left[\frac{\theta(t)}{t} \right]_+$ with

$$\int_0^t dt' \left[\frac{\theta(t')}{t'} \right]_+ = \log t \quad (5.4)$$

and the δ -distribution $\delta(t)$ with

$$\int_0^t dt' \delta(t') = 1. \quad (5.5)$$

Equating coefficients in $\int_0^t dt' B_{b/g}^{(1)}(t', x, \mu)$ then yields

$$\begin{aligned} B_{b/g}^{[5](1)}(t, x, \mu) &= \frac{\alpha_s}{2\pi} T_F \theta(x) \left[P_{gq}(x) \left(\frac{1}{\mu^2} \mathcal{L}_0 \left[\frac{t}{\mu^2} \right] + \delta(t) \left(\log \frac{1-x}{x} - \log \frac{m_b^2}{\mu^2} - 1 \right) \right) \right. \\ &\quad \left. + \theta(1-x) + \mathcal{O}\left(\frac{m_b^2}{t}\right) \right]. \end{aligned} \quad (5.6)$$

Thus we obtain for the matching coefficient at 1-loop level

$$\begin{aligned}\mathcal{I}_{bg}^{(1)[5]}(t, x, \mu_B) &= B_{b/g}^{[5](1)}(t, m_b, x, \mu_B) - \delta(t) f_{b/g}^{(1)[5]}(m_b, x, \mu_B) \\ &= \frac{\alpha_s}{2\pi} T_F \theta(x) \left[P_{gq}(x) \left(\frac{1}{\mu^2} \mathcal{L}_0 \left[\frac{t}{\mu^2} \right] + \delta(t) \left(\log \frac{1-x}{x} - 1 \right) \right) \right. \\ &\quad \left. + \theta(1-x) + \mathcal{O} \left(\frac{m_b^2}{t} \right) \right] \quad (5.7)\end{aligned}$$

where all the IR mass dependence cancels as expected. This result coincides with the matching coefficient given in [2] for the matching of massless beam functions (4.8) onto massless partonic PDFs (3.5), i.e. for $\mu_m \sim m_b \gg \sqrt{t} \sim \mu_B$. Here all contributions from interactions with momentum transfer $\gtrsim m_b$ are integrated out and this massless matching is the leading order contribution for the matching between massive quark PDFs and beam functions for $m_b^2 \ll t$.

In order to obtain the one-loop beam function $B_{b/g}(t, x, \mu_B)$ for $t \gg m_b^2$ one proceeds as described in chapter 2.2 using the matching coefficients in chapter 3.3 and 5

$$\begin{aligned}B_{b/g}^{[5](1)}(t, m_b, \mu_B) &= \mathcal{I}_{bb}^{(0)[5]}(t, \mu_B) \otimes \left(\mathcal{M}_{bg}^{(1)}(m_b, \mu_m) \otimes \left(f_{g/g}^{(0)[4]}(\mu_\Lambda) \right) \Big|_{\mu_\Lambda \rightarrow \mu_m} \right) \Big|_{\mu_m \rightarrow \mu_B} \\ &\quad + \mathcal{I}_{bg}^{(1)[5]}(t, \mu_B) \otimes \left(\mathcal{M}_{gg}^{(0)}(\mu_m) \otimes \left(f_{g/g}^{(0)[4]}(\mu_\Lambda) \right) \Big|_{\mu_\Lambda \rightarrow \mu_m} \right) \Big|_{\mu_m \rightarrow \mu_B}\end{aligned}$$

where the subscript $\mu_m \rightarrow \mu_B$ denotes the DGLAP evolution from μ_m to μ_B etc.. This beam function includes a resummation of logarithms $\log \frac{m_b^2}{t}$ to all orders of α_s but does not include power corrections $\mathcal{O} \left(\frac{m_b^2}{t} \right)$.

5.2.2 $t \sim m_b^2$

For the case $t \sim m_b^2$ the scale from which one has to consider the jet-like behavior of the initial state coincides with the scale at which the heavy b -quark becomes active. Thus one can directly match the massive beam function onto the partonic PDF in the 4FS. The matching equation at NLO is

$$\begin{aligned}B_{b/g}^{[4](1)}(t, m_b, \mu_B) &= \mathcal{I}_{bi}^{(0)[4]}(t, m_b, \mu_B) \otimes f_{i/g}^{(1)[4]}(\mu_B) + \mathcal{I}_{bi}^{(1)[4]}(t, m_b, \mu_B) \otimes f_{i/g}^{(0)[4]}(\mu_B) \\ &= \mathcal{I}_{bg}^{(1)[4]}(t, m_b, \mu_B)\end{aligned}$$

which is illustrated in Figure 5.3 and where the subscript [4] at $B_{b/g}^{(1)}$ is again only introduced in order to differentiate between both mentioned cases and does not mean that the beam function is evaluated in the 4FS. Here the sum over i is over the light quarks and gluons only. Thus we obtain for the matching coefficient

$$\mathcal{I}_{bg}^{(1)[4]}(t, m_b, x, \mu_B) = \frac{\alpha_s}{2\pi} T_F \theta(x) \left[P_{gq}(x) t + 2m_b^2 \theta(1-x) x^2 \right] \frac{\theta \left(\frac{1-x}{x} t - m_b^2 \right)}{t^2}. \quad (5.8)$$

For completeness, the contribution of Figure 4.5 with a massive fermion loop to $\mathcal{I}_{gg}^{(1)}$ gives

$$\mathcal{I}_{gg(Q)}^{[4](1)}(t, m_b, x, \mu_B) \Big|_{ML} = -\frac{\alpha_s}{\pi} \frac{4T_F}{3} \delta(t) \log \frac{\mu^2}{m_b^2} \delta(1-x), \quad (5.9)$$

5.4 Main Results of this Report

We calculated the massive partonic beam function at one-loop order (4.10) in section 4.3 and this result allowed us to find the NLO matching coefficient (5.8) for the matching between massive beam functions and massless PDFs in the regime $m_b^2 \sim t$. Including resummation of $\log \frac{m_b^2}{t}$ relevant for the regime $m_b^2 \ll t$ we also extended this result to arbitrary hierarchies between m_b and \sqrt{t} . These results are not known in literature yet and find application in heavy-quark induced processes e.g. in the $b\bar{b}H$ production with a jet veto.

Bibliography

- [1] I. Stewart, F. Tackmann, and W. Waalewijn. Factorization at the LHC: From PDFs to Initial State Jets. arXiv:0910.0467v3
- [2] I. Stewart, F. Tackmann, and W. Waalewijn. The Quark Beam Function at NNLL. arXiv:1002.2213v3
- [3] M. Bonvini, A. Papanastasiou, and F. Tackmann. Resummation and Matching of b -quark Mass Effects in $b\bar{b}H$ Production. arXiv:1508.03288v1
- [4] P. Pietrulewicz. Variable Flavor Number Scheme for Final State Jets.
- [5] C. Bauer, and I. Stewart. The Soft-Collinear Effective Theory. lecture notes